Geodesy and Geodynamics 15 (2024) 82–99

Contents lists available at ScienceDirect

Geodesy and Geodynamics

journal homepage: http://www.keaipublishing.com/geog

Geomorphic signatures and active tectonics in western Saurashtra, Gujarat, India

Bikramaditya Mondal [a], Mery Biswas [b], Soumyajit Mukherjee [a, *], Mohamedharoon A. Shaikh [a]

[a] Department of Earth Sciences, Indian Institute of Technology Bombay, Mumbai 400076, Maharashtra, India
[b] Department of Geography, Presidency University, Kolkata 700073, West Bengal, India

ARTICLE INFO

Article history:
Received 8 October 2022
Accepted 3 August 2023
Available online 2 September 2023

Keywords:
Active tectonics
Geomorphology
Western Saurashtra
Archeology
North kathiawar fault system

ABSTRACT

Active tectonics in an area includes ongoing or recent geologic events. This paper investigates the tectonic influence on the subsidence, uplift and tilt of western Saurashtra through morphotectonic analysis of ten watersheds along with characteristics of relief and drainage orientation. Watersheds 7–9 to the north (N) are tectonically active, which can be linked with the North Kathiawar Fault System (NKFS) and followed by watersheds 6, 10, 1, 4 and 5. Stream-length gradient index and sinuosity index indicate the effect of tectonic events along the master streams in watersheds 6–9. Higher R^2 values of the linear curve fit for watershed 7 indicate its master stream is much more tectonically active than the others. The R^2 curve fitting model and earthquake magnitude/depth analysis confirm the region to be active. The reactivation of the NKFS most likely led to the vertical movement of western Saurashtra.

1. Introduction

The Saurashtra (Kathiawar) peninsula of the Gujarat state (India) dominantly consists of Deccan basalts, while the coastal region is constituted of Cenozoic sediments [1]. The Saurashtra region has classically been considered a pericratonic basin [2]. Saurashtra is a fault-bound plateau with an overall radial slope. The peninsula has been considered to be neotectonically inactive for a long period [3]. Nevertheless, studies in the last few decades revealed its recent tectonic activities [2–4]. For example, earthquakes were recorded from August 9, 2000 to December 15, 2000 at Bhavnagar, eastern Saurashtra [4]. Geochronologic and morpho-stratigraphic studies of the coastal belts of Saurashtra indicate that its neotectonics is at least 125 ky old [5,6].

The Indian city Dwarka is located near the western tip of the Saurashtra peninsula (Fig. 1). The southern fringe of the Gulf of Kutch is occupied by the landmass Bet Dwarka/Bet Sankhodar ("Bet"/"Beyt" means "island") (Fig. 1). The area is characterized by Cenozoic clastics and carbonates [7]. Bet Dwarka was possibly connected with mainland Saurashtra about 2000 years back and got inundated and detached from the mainland approximately 1000 years ago [8]. Offshore of Dwarka used to be an ancient port. There is evidence of several important maritime activities that continued till the late medieval period (about late 5th - late 15th centuries) [9]. Unlike the western boundary of the Indian subcontinent, Dwarka, Bet Dwarka and the surrounding areas were affected by the Late Cenozoic sea level changes [9–16] (detail in Appendix 1). The sea level fluctuation curve for the western Indian continental margin [10] matches the global sea level fluctuation history after the last glacial maxima [17,18]. This indicates that the sea level rise here was in response to a global phenomenon. One can expect a tectonic component in sea-level fluctuation, which contributed to the submergence during the Holocene Period. This is because the Saurashtra area is partly fault-bound and seismic as well. The Tectonics of Saurashtra is inherently linked with the Harappan civilization and the submergence of the mythological city Dwarka. Therefore, Saurashtra's tectonics attracts multidisciplinary interest.

* Corresponding author.
E-mail addresses: soumyajitm@gmail.com, smukherjee@iitb.ac.in (S. Mukherjee).

Peer review under responsibility of Institute of Seismology, China Earthquake Administration.

Production and Hosting by Elsevier on behalf of KeAi

https://doi.org/10.1016/j.geog.2023.08.001

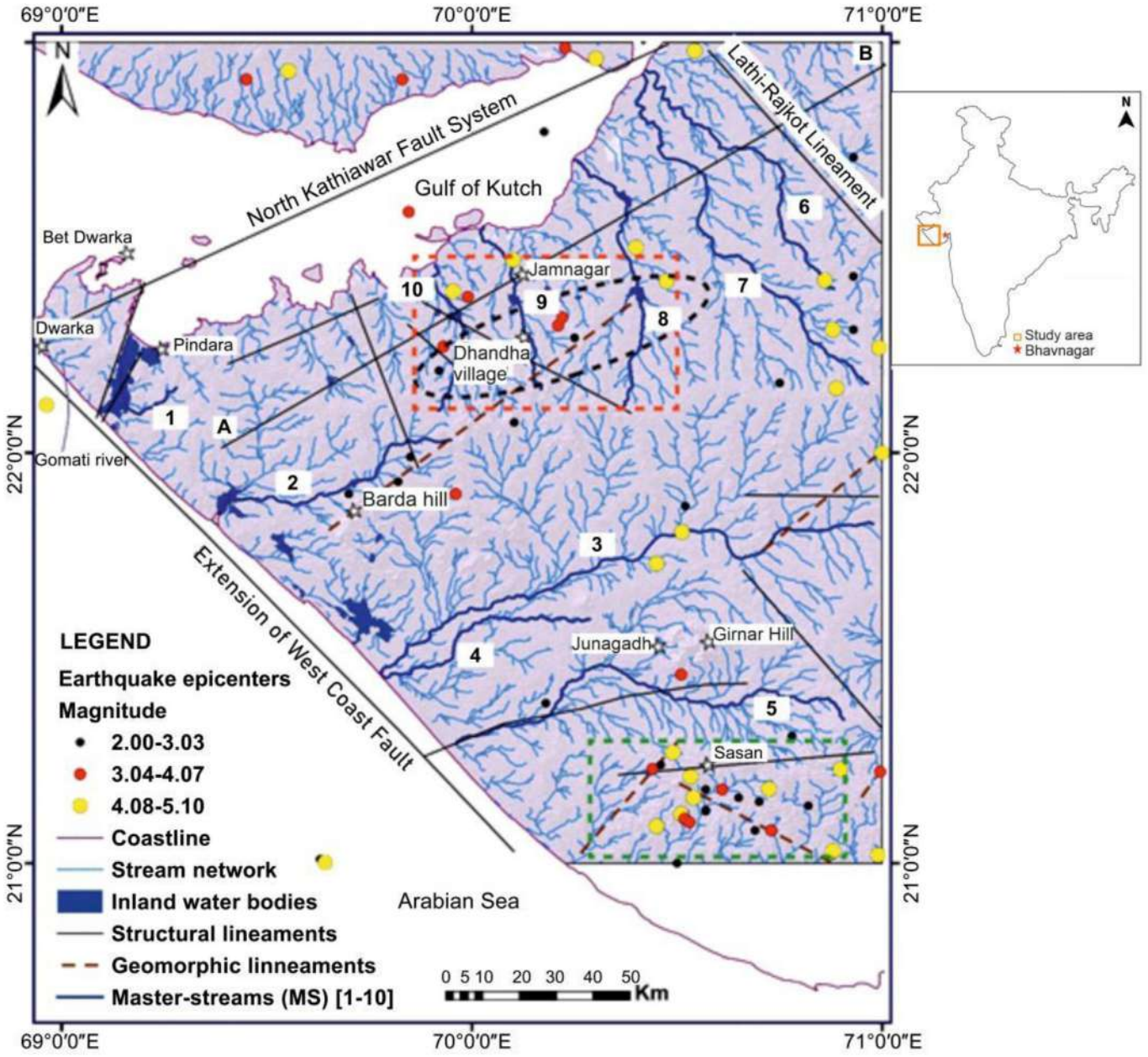

Fig. 1. Major structural lineaments, faults and geomorphic lineaments [19–21]. Line AB represents a fault [17]. Black dotted ellipse indicates the zone of rejuvenation [21]. Drainage is extracted from the digital elevation model (Shuttle Radar Topographic Mission, acquired on Februray 11, 2000, published on September 23, 2014). Colored circles are earthquake epicenters from 1872 to 2021 [22]. Circles with the smallest radius in blue, intermediate radius in red and largest radius in light yellow denote earthquake magnitude ranges 2.00–3.03, 3.04–4.07 and 4.08–5.10, respectively. Ten major channels (deep blue) indicate the master streams (MS). The green dot in the inset is the transpression regime [4]. Red and green dashed rectangles are dominated by reverse faults. The reverse faults indicate compression along ESE-WNW and transtension related to NE-SW strike-slip faults [21,23,24]. GOC: Gulf of Cambay/Khambat. Previous morphometric works can be found in Refs. [25–27].

Geomorphic parameters can assess the active tectonics in Saurashtra. Few geomorphic studies have been performed by the previous workers in Saurashtra, but with different aims than this work (Table 1). Previous researches did not investigate the entire study area of this article in terms of watersheds and morphometric parameters at linear and spatial scales.

Kandregula et al. worked with merely six basin-scale parameters for the northern watersheds of Saurashtra [26]. Further, Gandhi et al. studied the drainage anomalies of five watersheds from western Saurashtra [27]. In these works, no long profile curves were fitted to R^2 model, nor were any watershed-scale comparisons of morphometric parameters performed. Few major faults have been delineated in Saurashtra by the previous workers [26], and recent tectonic events, e.g., the uplift and submergence of Saurashtra's western portion, remain poorly understood. As one of the significant sections of the Indian continental lithosphere, the Saurashtra Peninsula has interesting geophysical anomalies and has experienced tectono-thermal modification since the Mesozoic period. In-depth studies are required to understand the seismo-tectonics and morphotectonics of the entire Saurashtra [26].

The current study aims to examine the drainage characteristics through morphometric analysis of ten watersheds of the Saurashtra area (Fig. 2). This work utilizes the Index of Active Tectonics (IAT) to evaluate and categorize the watersheds [28]. We evaluate nine

Table 1
Previous geomorphic works in and around the study area and the key results.

References	Terrain	Approaches	Key results
Ref. [27]	Southwestern Saurashtra	Analysis of morphometric indices using GIS	1. Southern region (of southwestern Saurashtra) is the most tectonically active zone.
Ref. [18]	Entire Saurashtra	Remote sensing and analysis of morphometric indices using GIS	1. Predicting a fault AB (Fig. 1); 2. Northern Saurashtra is tectonically active with a dextral strike-slip regime with a rotational component manifesting tilting of the northern block towards east.
Ref. [26]	Northern Saurashtra	Analysis of morphometric indices using GIS and correlation with earthquake epicenter locations	1.39.5% area of northern Saurashtra is active and 44% area is very active.
Ref. [21]	Eastern and Northern Saurashtra	Correlation of tectonic information and geomorphic information (analysis morphometric indices using GIS)	1. Identifying an ENE-WSW trending zone of rejuvenation in Northern Saurashtra (Fig. 1); 2. An active subsurface structural feature along the same trend.

morphometric indicators at the basin-scale. The linear-scale parameters were also utilized that specify the tectonic imprint along the ten master streams of the watersheds. Based on the R^2 model, tectonically sensitive master streams of the terrain were identified and prioritized with ranks. Thus, the work includes (i) morphometric analysis for assessing active tectonics of watersheds (basin-scale) and streams (liner-scale) and (ii) seismologic overview of the study area.

2. Study area

2.1. General points

Rocks of Tertiary crop out at the westernmost portion of the Saurashtra peninsula, including Okha, Dwarka, Bet Dwarka and the surroundings [19] (Fig. 3 and Table 2). The ancient city Dwarka is located at the westernmost tip of the Saurashtra mainland (Fig. 3). The Bet Dwarka island occupies the southern fringe of the Gulf of Kutch (Fig. 3), which is possibly a continuation of the mainland Saurashtra. However, to understand the effect of active tectonics, an extended region was selected for the study (Figs. 1 and 2). The Bet coast (located approximately 3 km away from the Okha coast) (Fig. 3) is about 13 km long NW-SE strip and about 4 km wide [27]. The island is nearly 36 km^2 with about 8 m elevation from the mean sea level [18]. The northwest part of the area is a low-lying portion with fine beach sands. On the other hand, the southeastern part of the beach comprises clayey materials with high cliffs [29]. The eastern part of the Bet contains sand hills and bushes. The southwest part has an elevation of about 20 m [12]. The Dwarka region mainly comprises recrystallized fossiliferous Kalyanpur Limestone Member and sandy Lower Pliocene limestone [29] (Fig. 3). Table 2 presents the major lithology and stratigraphic succession of the westernmost part of the Saurashtra area.

The study area is located at 21° N to 23° N and 69°E to 71°E (Fig. 2). Ten major master streams flowing in different directions contribute significantly to the denudational landforms. Northerly flowing master stream formed watersheds with an overall S-N trend, and those flowing westerly developed E-W trending watersheds.

2.2. Geomorphology and geology

Saurashtra is mainly characterized by rugged erosional topography with linear ridges having several plutonic complexes of different compositions and abundant dykes [30]. Appendix-2 presents the major geomorphologic divisions. The region consists of hills, pediment/alluvial plains and mud-flats. Hills mainly consist of Deccan trap basalts.

The tectonic structure of Saurashtra is influenced by the interplay of the three Precambrian tectonic grains: Dharwar (NNW-SSE), Aravalli-Delhi (NE-SW) and Satpura (ENE-WSW) [1,30]. The faults and lineaments are (sub)parallel to the major grains [31] (Fig. 2). These grains define the region as a fault-bound horst.

The northern limit of the study area is marked by the North Kathiawar Fault System (NKFS). NW-trending extension of the West Coast Fault parallels the coastline and defines the western limit (Fig. 1) [30]. Different tectonic phases affected the regions while the Indian plate rifted and subsequently drifted northward [30,32–35]. There are two unnamed NNE-SSW and NE-SW trending faults bounding the Okha raan [7,19] (Fig. 3).

Regional maximum horizontal stress axis from the interpreted borehole breakout data of the offshore Kutch-Saurashtra basin trends NNE under a strike-slip regime (from World Stress Map in Ref. [36]). Other authors' conclusions, e.g., different stress orientations in different places [24], conflict in this regard.

3. Present work

3.1. Data & methodology

Shuttle Radar Topographic Mission (SRTM) Digital Elevation Model (DEM) with 30 m × 30 m spatial resolution was used to extract drainage, delineate and analyze watersheds and calculate morphometric indices. The data does not contain cloud cover. Hence atmospheric correction was not needed. Different areal, relief and linear parameters were calculated using ArcGIS (version 10.3, 2014).

D8 Python algorithm for the required threshold value was used to generate and extract the stream network. It includes demarcation of the flow path. Slope directions were deduced from each pixel to its eight-neighbor pixels.

Nine morphometric indices were calculated to understand the tectonic activeness of the entire region. The geomorphic indices of nine parameters and the Index of Active Tectonics (IAT) were calculated for watersheds 1–10. Linear morphometric parameters of each river were evaluated to correlate with the structural elements. To better understand the effects of tectonics, curve fitting was also performed for four functions: linear, exponential, logarithmic and power of longitudinal profiles. Fig. 4 presents the methodologies used in this study. Specific locations in watershed 9 were surveyed in the field. Thus, both the primary field data and secondary DEM data were utilized.

3.2. Relief and areal parameters and IAT analysis

Relief parameters, i.e., ruggedness number (H_d), relief ratio (R_h), hypsometric integral (HI), and areal parameters, i.e., asymmetry factor (AF), circularity ratio (R_c), elongation ratio (R_e), form factor (R_f), basin shape (B_s) and transverse topographic symmetry factor (T) were calculated for all the watersheds (Tables 3 and 4). These were used to calculate the IAT, indicating the relative tectonic

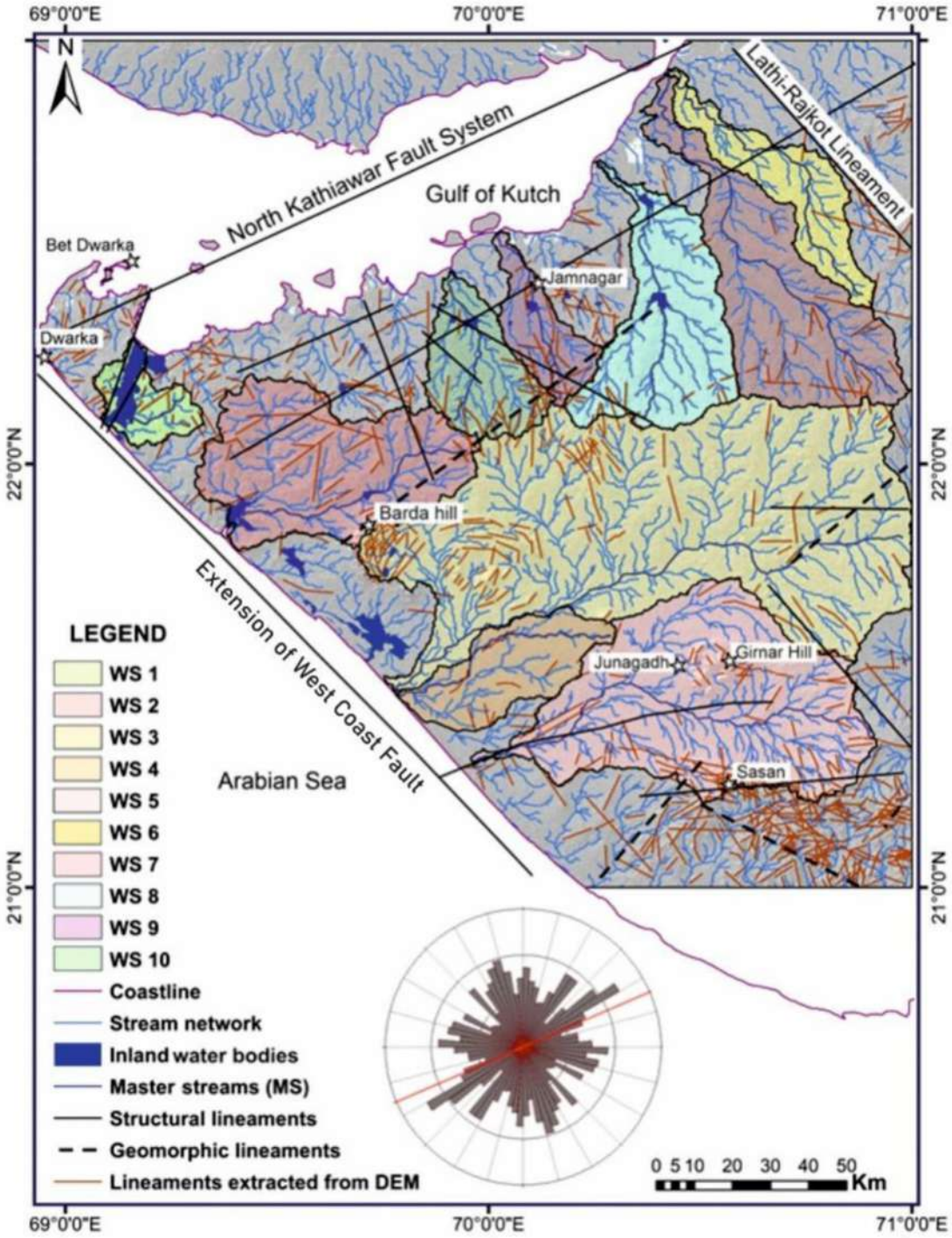

Fig. 2. Ten watersheds (WS). The 698 lineaments are identified from the digital elevation model (DEM). Previously known lineaments [3] are also plotted. The rose diagram is generated by RockWorks 20 software, 2022.

activities. For example, the asymmetry factor is a crucial parameter for determining how much a river basin has tilted tectonically. The main stream modulates its course and slopes away from the midline of the basin. Table 3 defines the morphometric parameters.

IAT reliably evaluates the relative degree of tectonic activeness [43–46]. IAT results quantitatively define the geomorphic and drainage characters [47]. IAT values can be classified into certain ranges to understand the relative tectonic activity [45,46]. The individual morphometric parameters were clubbed as class 1 (maximum tectonic influence), class 2 (moderate tectonic influence) and class 3 (minimum tectonic influence).

3.3. Linear parameters

These parameters (Table 4) are correlated with the position of structural elements (faults and lineaments). The tectonic morphometry includes Stream-length (SL) gradient index and Sinuosity Index (SI) analyses [48] to examine the tectonic

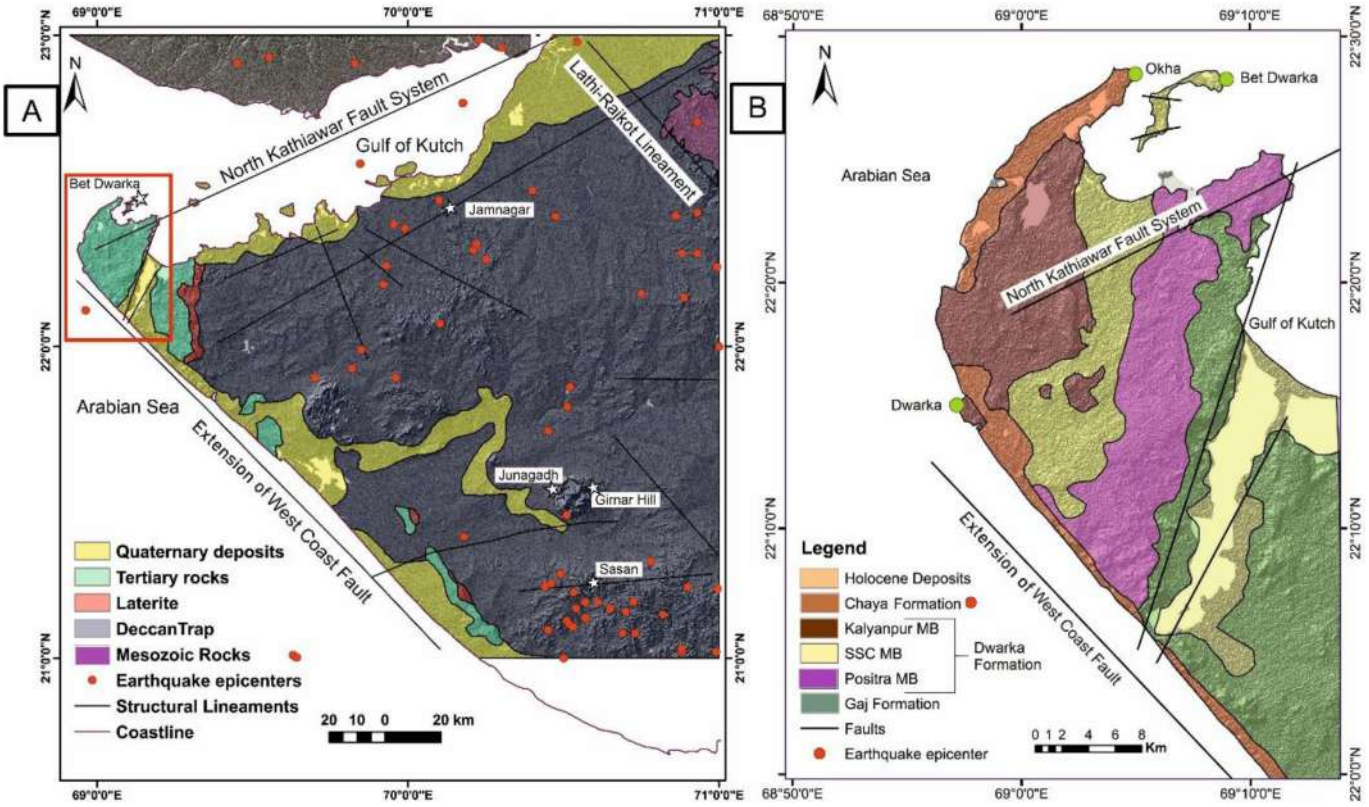

Fig. 3. (A) Geologic formations with faults/lineaments and earthquake points of the study area [17,25]. (B)Major structural and stratigraphical elements of Dwarka, Bet Dwarka and surrounding areas [7,20].

Table 2
Detailed lithostratigraphic classification of the Saurashtra area Dwarka, Bet Dwarka and surrounding areas, compiled from a-Ref. [32], b-Ref. [7], c-Ref. [19].

Age	Formation	Member (thickness)	Lithology
Holocene	Holocene Deposits		Beach and dune sands, tidal clays and Alluvium[b,c]
Late Pleistocene to Holocene	Chaya Formation	Armada Reef Member (4 m)[b,c]	Coral Reef limestone[b,c]
Middle to late Pleistocene	Chaya Formation	Okha Shell Limestone Mb. (10 m)[b,c]	Bioclastic limestone[b,c]
Lower Pleistocene	Dwarka Formation	Kalyanpur Limestone Member (30 m)[b,c]	Recrystallized fossiliferous limestone[b,c]
Upper Miocene	Dwarka Formation	Sankhodhar Sand- Clay Member (60 m)[b,c]	Tidal rhythmites, hummocky cross-stratification[c]
		(Tidal environment of	Flat pebble conglomerate[a]
		Pleistocene high sea level)[a]	Siltstone[c]
			Fine-grained cross stratified sst.[b]
			Flat pebble conglomerate[c]
			Sandy clay and sst.[b,c]
Middle Miocene	Dwarka Formation	Positra Limestone (25 m)[b,c]	Bioclastic and coralline limestone with few dolomitic bands[b,c]
Lower to middle Miocene	Gaj Formation	Ranjitpur Limestone (5 m)[b,c]	Yellow fossiliferous limestone[b,c]
		Ashapura Clay Member (90 m)[b,c]	Clay, marls, and Gypsum bands[b,c]

signatures on drainage patterns. Each master stream of the ten watersheds was divided into ten segments, and the SL index and SI were calculated for each segment separately.

3.4. Analysis of the best-fit curve of longitudinal profiles of master streams

Normalized longitudinal profile models can be developed by these equations [51]:

$$\text{Linear function} : y = ax + b \quad (1)$$

$$\text{Exponential function} : y = ae^{bx} \quad (2)$$

$$\text{Power function} : y = ax^b \quad (3)$$

$$\text{Log function} : y = a \ln x + b \quad (4)$$

Here a and b are coefficients derivable from each profile, and the results will be different due to different data sets.

The above four functions of a normalized longitudinal profile can portray the tectonic effect on rivers [52]. Based on the maximum values of R^2 for fitting linear, exponential, logarithmic and power curves, watersheds were categorized as per their tectonic activity as very high, high, moderate, and low [52].

Two longitudinal profiles of watersheds 6 and 7 have higher R^2 curve fitting values in linear than those with other R^2 values of

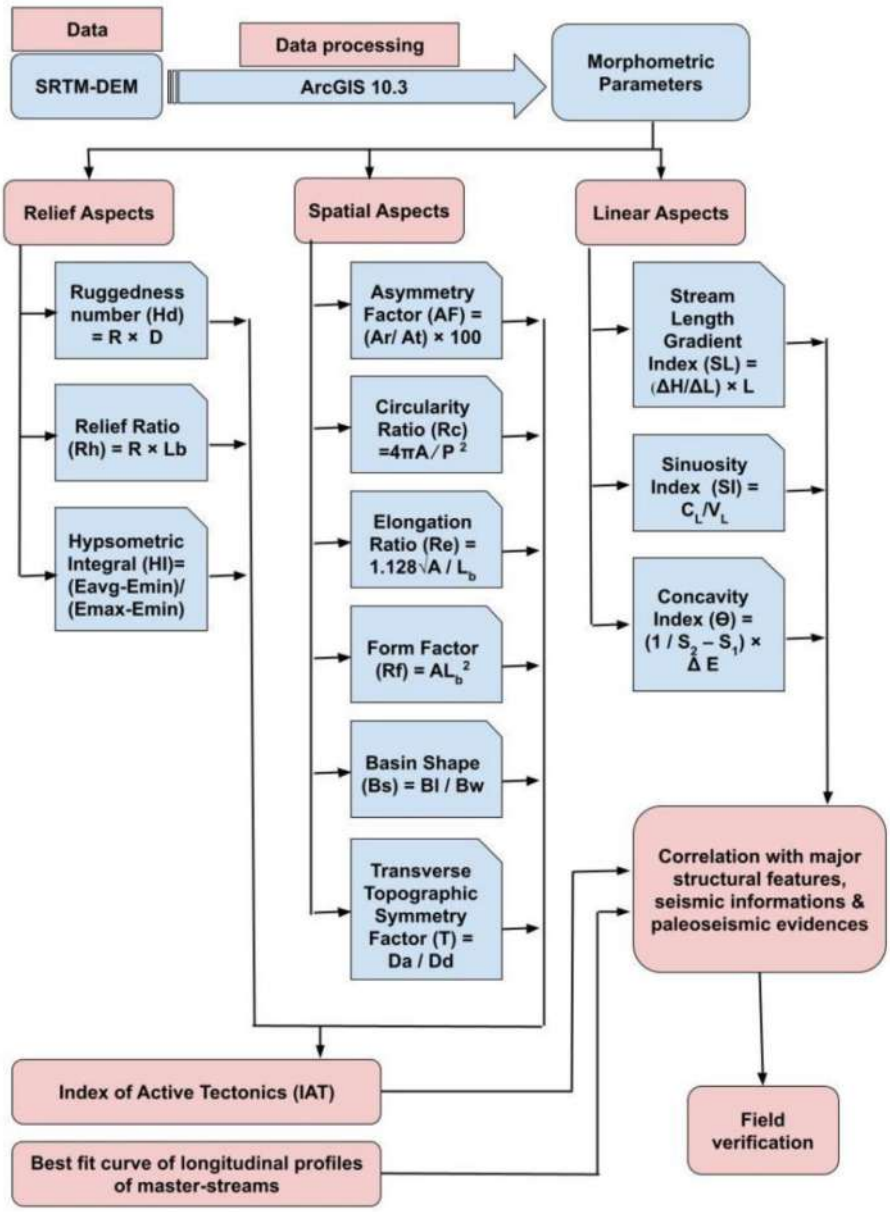

Fig. 4. Flow chart of methodologies in this work.

exponential/logarithmic and power functions, indicating their trend of tectonic activeness. To define the activeness difference between the highest values of R^2 for any function (linear/exponential/logarithmic/power), the respective master streams were considered. The differences in R^2 values of each master stream (MS) were further ranked to assess tectonic control.

H is the elevation (m) of each intersecting point with respect to mean sea level (MSL). H_0 represents the source point of the elevation (m) of the river. As per Eqs. (1)–(4), $y = H/H_0$. L represents the distance between the source point of the river and the considered point. L_0 is the total length (km) of a river, according to Eqs. (1)–(4):

$$x = L\,L_0^{-1} \tag{5}$$

The coefficient of correlation (R^2) determines the degree of fit [43]. The curve having the highest value of R^2 indicates the best-fit curve. The difference between the value of linear R^2 and the highest R^2 deduced from Eqs. (2)–(4) indicates how tectonics influenced different master streams. The less the difference, the more the influence of the recent tectonic activity.

Different geomorphic parameters connote active tectonics (Table 4). In tectonically active regions, such as the southwest United States [53,54], Costa Rica [55], the Oregon Coast Range in the United States [56], the Kutch region in India [57], the Jaisalmer and the Barmer basins in Rajasthan, India [44,45], southeast Spain [58] and western Taiwan of China, all these considered geomorphic indicators were used. The channel's shape is changed in response to the surplus flow and sediments as per the basin's lithology, climate, rainfall and other pertinent factors [39,41,59].

Table 3
Definition of geomorphic indices. sl. 1–3: relief parameters; sl. 4–9: areal parameters.

Sl.No.	Parameters	Formula	Meanings of symbols	References
1	Ruggedness number (H_d)	$R \times D$	R = Basin relief D = Drainage density of the basin	Ref. [37]
2	Relief ratio (R_h)	R/L_b	R = Basin relief L_b = length of the basin	Ref. [38]
3	Hypsometric integral (HI)	$\frac{(\mathrm{Ele_{avg}} - \mathrm{Ele_{min}})}{(\mathrm{Ele_{max}} - \mathrm{Ele_{min}})}$	$\mathrm{Ele_{avg}}$ = Average of elevation $\mathrm{Ele_{min}}$ = Minimum elevation $\mathrm{Ele_{max}}$ = Maximum elevation	Ref. [39]
4	Asymmetry factor (AF)	$(A_{r/}A_t) \times 100$	A_r= Area of the Basin to the right of the master stream facing downstream A_t = Total area of the basin	Ref. [40]
5	Circularity ratio (R_c)	$4\pi A/P^2$	A = Area of the basin $\Pi = 3.14$; P = Perimeter of the basin	Ref. [41]
6	Elongation ratio (R_e)	$1.128\sqrt{A}/L_b$	A = Area of the basin L_b = Length of the basin	Ref. [31]
7	Form factor (R_f)	A/L_b^2	A = Area of the basin L_b^2 = Square of basin length	Ref. [41]
8	Basin shape (B_s)	B_l/B_w	B_l = Basin length from Head point to mouth B_w = Width of the basin	Ref. [42]
9	Transverse topographic symmetry factor (T)	D_a/D_d	D_a = Distance from the active meander-belt mid-line to the basin midline D_d = Distance from the basin divide to the basin midline	Ref. [43]

Table 4
Formulae and description of linear parameters.

Sl. No.	Parameters (unit)	Formula	Meaning of symbols	References
1	Stream-length gradient index (SL) (m)	$(\Delta H/\Delta L) \times L$	ΔH = Difference in altitude ΔL = Length of the reach L = horizontal length from watershed divide to the midpoint of the reach	Ref. [49]
2	Sinuosity index (SI) (unitless)	C_l/V_L	C_L = channel length between two points on a river V_L=valley length (straight line distance between the same two points)	Ref. [50]
3	Concavity Index (Θ) (unitless)	$1/(S_2 - S_1) \times \Delta E$	S_1 = Channel slope before disturbance, S_2 = Channel slope after disturbance (e.g., due to a change in incision rate E) ΔE = Difference between the incision rate before and after disturbance.	Ref. [51]
4	Normalized Steepness index (K_{sn}) (unitless)	$k_s A^{\Theta}$	k_s characterizes channel steepness and θ indicates the concavity of the river channel, which are referred to as the channel steepness index and the channel concavity index, respectively.	Refs. [51,52]

4. Results

4.1. Areal and relief parameters

The areal and the relief parameters were determined to analyze topography, steepness, erosion rate, etc. These parameters were used to calculate the IAT.

Table 5 shows that the ruggedness number (H_d) of all the watersheds varies from 0.07 to 0.42. The study reveals the relief ratio (R_h) from 0.002 to 0.03 for all the ten watersheds. Hypsometric integral (HI) in the ten watersheds ranges from 0.472 to 0.504. AF varies from 37% to 80% for the ten watersheds. The normalized value |50-AF| varies from 0.03 to 0.30 for all the watersheds. Values of R_c for all the watersheds range from 0.15 to 0.33, which were further clubbed into three groups.

In the study area, R_e varies from 0.41 to 0.82, R_f ranges from 0.13 to 0.53, B_s lies between 1.4 and 4.7, and T ranges from 0.16 to 0.5 (Table 5). Higher values of H_d, R_h, normailized AF, HI, B_s and T

Table 5
Evaluated values and classification of basin-scale parameters for the watersheds (WS) [44,45].

Watershed	Ruggedness number (H_d)	Relief Ratio (R_h)	Asymmetry factor (AF) Normalized	Hypsometric Integral (HI)	Circularity Ratio (R_c)	Elongation Ratio (R_e)	Form Factor (R_f)	Basin Shape (B_s)	Trans.Topo. Sym Factor (T)
WS 1	0.33	0.030	0.13	0.490	0.31	0.82	0.53	1.8	0.31
WS 2	0.21	0.010	0.19	0.485	0.30	0.80	0.51	1.4	0.38
WS 3	0.21	0.004	0.29	0.480	0.22	0.72	0.41	1.7	0.50
WS 4	0.11	0.004	0.25	0.472	0.33	0.61	0.29	2.6	0.50
WS 5	0.42	0.011	0.04	0.477	0.28	0.67	0.35	1.8	0.16
WS 6	0.07	0.002	0.03	0.494	0.15	0.41	0.13	4.7	0.36
WS 7	0.10	0.003	0.30	0.495	0.18	0.51	0.21	2.5	0.46
WS 8	0.08	0.005	0.13	0.499	0.22	0.68	0.37	1.6	0.42
WS 9	0.09	0.005	0.03	0.504	0.25	0.54	0.23	2.6	0.49
WS 10	0.10	0.006	0.11	0.490	0.31	0.68	0.36	1.6	0.39
Classification									
Class 1	0.31–0.43	≥0.010	0.21–0.30	0.496–0.507	0.15–0.21	0.41–0.54	0.12–0.25	≥2.1	0.39–0.52
Class 2	0.18–0.30	0.005–0.009	0.11–0.20	0.484–0.495	0.22–0.28	0.55–0.68	0.26–0.39	1.6–2.0	0.27–0.38
Class 3	0.05–0.17	0.000–0.004	0.01–0.10	0.472–0.483	0.29–0.35	0.69–0.82	0.40–0.53	1.1–1.5	0.15–0.26

indicate higher tectonic influence, whereas higher values of R_c, R_e and R_f connote lesser impact.

4.2. Linear parameters

SL index and SI were computed for each segment for all master streams (Tables 6 and 7), respectively. The concavity index of each master stream for the ten watersheds was evaluated to correlate with the active tectonic zones (Table 1).

4.3. Analysis of best-fit curve of longitudinal profiles of master streams

Table 8 documents the R^2 values of four functions of the normalized longitudinal profiles. The differences between the highest R^2 values of the exponential, logarithmic and power curves compared to the linear R^2 values help to rank the master streams as per the tectonic influence on them.

5. Discussions

The drainage pattern follows the slope direction. For example, watershed 3 with the maximum number of streams shows the dominant slope direction to be NW and S to SE. Overall, the area is characterized by a very low slope (0–1.65°) besides a few elevated areas, such as around Girnar and Barda hills.

The Girnar hill within watershed 5 is characterized by a centrifugal drainage pattern (Fig. 5). This confirms a domal structure at Girnar hill. Multiple flow directions exist in the Barda hill region, which is part of watershed 3. These flow paths following lineaments define a complicated barbed pattern supported by a slope up to 75° [59,60]. The master stream of watershed 5 is fault-guided, since it flows along the structural lineament of the Girnar Hill. Watershed 2 is dominantly characterized by a rectangular drainage pattern (Fig. 5), which connotes an orthogonal network of brittle planes [60]. The stream network in watershed 2 trends NE-SW and follows a structural lineament (AB in Fig. 1) parallel to the NKFS. Another geomorphic lineament parallels the NKFS (Figs. 1, 2 and 7). These figures demonstrate that the stream network at watershed 2 follows the NE- SW trend of two structural lineaments, one of which parallels the NKFS (AB in Fig. 1).

Lower-order streams flow in a subcircular/concentric pattern (annular drainage). The northern portion of watershed 4 is characterized by a series of ridge-valley structures (Fig. 5). It defines a pinnate drainage pattern.

For the northern watersheds of Saurashtra, Kandregula et al. only used six basin-scale factors in their study [26]. Gandhi et al. also investigated the drainage irregularities in five watersheds in western Saurashtra [27]. Results of morphometric parameters show that there was less tectonic activity during the Quaternary.

Table 7
Sinuosity index (SI) of segmented master streams of ten watersheds.

Master stream	S1	S2	S3	S4	S5	S6	S7	S8	S9	S10
MS 1	1.31	1.18	1.23	1.32	1.33	1.08	1.00	1.05	1.05	1.06
MS 2	1.12	1.25	1.25	1.17	1.06	1.14	1.19	1.27	1.42	1.34
MS 3	1.09	1.17	1.40	1.10	1.16	1.14	1.19	1.24	1.22	1.24
MS 4	1.28	1.30	1.27	1.25	1.19	1.31	1.14	1.17	1.35	1.20
MS 5	1.35	1.17	1.17	1.12	1.12	1.12	1.12	1.23	1.14	1.17
MS 6	1.16	1.22	1.22	1.11	1.22	1.14	1.19	1.36	1.56	1.54
MS 7	1.18	1.09	1.12	1.07	1.27	1.17	1.08	1.25	1.54	1.26
MS 8	1.17	1.16	1.10	1.07	1.06	1.06	1.14	1.26	1.17	1.31
MS 9	1.29	1.19	1.48	1.16	1.05	1.26	1.18	1.12	1.12	1.39
MS 10	1.25	1.24	1.06	1.09	1.25	1.09	1.13	1.05	1.06	1.36

5.1. IAT analysis

For the assessment of IAT, all the morphometric parameters are grouped into three classes (Table 5): class 1 (high), class 2 (moderate) and class 3 (low).

Tables 5, 9 and 10 show that higher H_d for watersheds 1 and 5 signifies an unstable region, and 0.31–0.43 is the computed class 1 range for these watersheds. The lower H_d values (0.05–0.17) of watersheds 4 and 6–10 indicate the least tectonic influence (class 3). H_d within 0.18–0.30 for watersheds 2 and 3 shows that these watersheds are tectonically influenced. For watersheds 3, 4, 6 and 7, the R_h values are low, which suggests that these watersheds are generally less steep (class 3). Watersheds 8–10 display intermediate R_h (0.005–0.009) that reveals a modest steepness (class 2). In contrast, watersheds 1, 2 and 5 belonging to class 1 have a greater R_h value (0.010). This denotes stepper terrains with greater tectonic inputs.

Watersheds 8 and 9 belonging to class 1 have higher HI (0.496–0.507), indicating the development of recent landforms due to active tectonics. These two watersheds are followed by watersheds 1, 2, 6, 7 and 10, which are moderately active belonging to class 2. HIs for these watersheds range from 0.484 to 0.495. Watersheds 3, 4 and 5 under class 3 with lower HI (0.472–0.483) indicate significantly less tectonic influence (Table 5).

For watersheds 3, 4 and 7, normalized AFs are0.29, 0.25 and 0.3, respectively, indicating more tectonic tilting (class 1) than watersheds 1, 2, 8 and 10 (class 2). In watersheds 5 and 6, very low normalized AFs are 0.04 and 0.03, respectively, indicating almost no tectonic tilting (class 3). As per the lower R_c values (0.15–0.21), watersheds 6, 7 and 8 are elongated. This suggests that there may have been tectonic activity (class 1). Watersheds 1, 2, 4 and 10 have higher values, indicating a more elliptical character of watersheds

Table 6
Evaluated values of SL index (m) of segmented master streams (MS).

Master stream	S1	S2	S3	S4	S5	S6	S7	S8	S9	S10
MS 1	4.00	6.90	7.50	15.75	9.90	13.75	9.75	0.01	0.01	1.90
MS 2	21.75	38.69	56.00	55.30	45.45	42.90	35.10	47.24	45.04	2.85
MS 3	9.10	0.60	44.25	65.43	55.78	0.55	63.03	50.98	58.63	47.49
MS 4	8.75	19.05	17.75	18.20	22.50	13.75	18.21	20.25	12.75	20.90
MS 5	37.46	85.49	77.48	71.36	72.49	38.50	58.49	67.09	40.37	28.50
MS 6	15.23	34.78	44.23	61.57	82.31	62.67	0.65	67.47	37.38	18.99
MS 7	19.20	40.94	50.24	46.54	95.82	42.89	42.89	45.74	43.34	18.99
MS 8	14.29	40.49	53.54	31.14	56.70	68.75	42.25	20.25	71.39	80.74
MS 9	19.70	57.59	45.25	74.90	50.40	62.15	60.45	64.60	64.60	41.80
MS 10	10.80	20.55	44.25	60.55	63.90	36.89	67.60	33.75	39.95	51.30

Table 8
Evaluated curve-fitting R^2 values of master streams of the ten watersheds. Black bold font: the differences between the highest R^2 values and the linear R^2 values.

Master stream	Linear R^2	Exponential R^2	Logarithmic R^2	Power R^2	Highest R^2 -Linear R^2	Rank
MS 1	0.8029	0.9723	0.8536	0.0119	**0.1694**	8
MS 2	0.8651	0.9881	0.9277	0.0241	**0.1230**	6
MS 3	0.9485	0.9540	0.8499	0.0275	**0.0055**	2
MS 4	0.8675	0.9917	0.9190	0.0056	**0.1242**	7
MS 5	0.8204	0.9967	0.9201	0.0019	**0.1763**	9
MS 6	0.9480	0.6625	0.8632	0.0020	**0**	1
MS 7	0.9177	0.9012	0.9001	0.0063	**0**	1
MS 8	0.9239	0.9630	0.8746	0.0022	**0.0391**	4
MS 9	0.8937	0.9478	0.8822	0.0031	**0.0541**	5
MS 10	0.9493	0.9565	0.8163	0.0036	**0.0072**	3

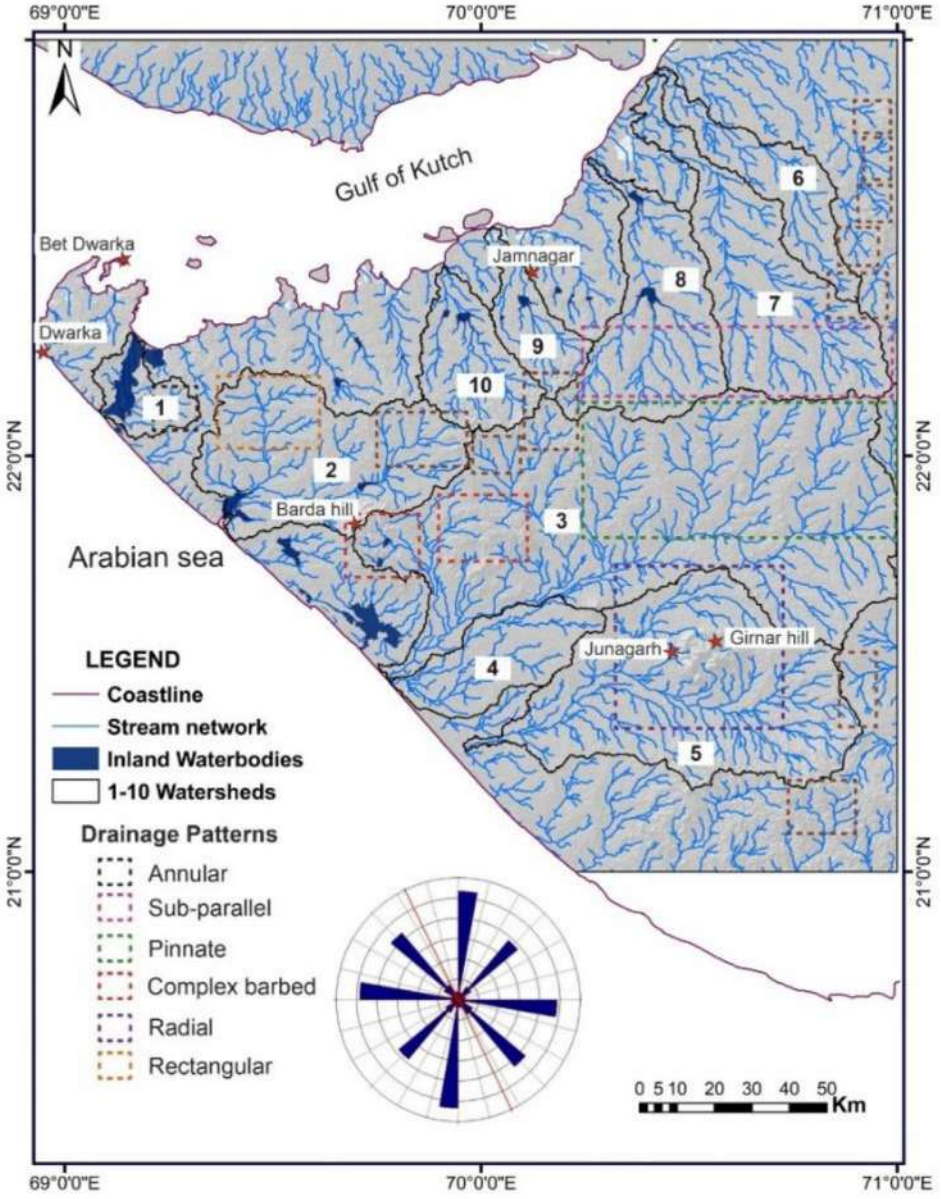

Fig. 5. Drainage patterns reveal the tectonic and topographic control on channel orientation. Rose diagram indicates the distribution of flow directions (using Rock Works 20 software, 2022).

(class 3). This is followed by elongated watersheds 3, 5 and 9 (class 2) (Tables 5, 9 and 10). R_e ranging from 0.69 to 0.82 for the watersheds 1, 2 and 3 allots them into class 3 (low activity), watersheds 4, 5 and 10 with R_e (0.55–0.68) are classified as class 2 (moderate activity), and watersheds 6, 7 and 9 with R_e (0.41–0.54) are classified as class 1 (active). The tectonic activeness was also measured

Table 9
Ranking of calculated values for the assessment of IAT.

Watershed	Ruggedness number (H_d)	Relief Ratio (R_h)	Asymmetry factor (AF) Normalized	Hypsometric Integral (HI)	Circularity Ratio (R_c)	Elongation Ratio (R_e)	Form Factor (R_f)	Basin Shape (B_s)	Trans. Topo. Sym Factor (T)	IAT
WS 1	1	1	2	2	3	3	3	2	2	2.11
WS 2	2	1	2	2	3	3	3	3	2	2.33
WS 3	2	3	1	3	2	3	3	2	1	2.22
WS 4	3	3	1	3	3	2	2	1	1	2.11
WS 5	1	1	3	3	2	2	2	2	3	2.11
WS 6	3	3	3	2	1	1	1	1	2	1.89
WS 7	3	3	1	2	1	1	1	1	1	1.56
WS 8	3	2	2	1	1	2	2	2	1	1.78
WS 9	3	2	3	1	2	1	1	1	1	1.67
WS 10	3	2	2	2	3	2	2	2	1	2.11

by magnitudes of R_c. For example, watersheds 6, 7 and 8 belong to class 1 (R_c equals to 0.15–0.21). Watersheds 2, 5 and 9 come under class 2 (R_c equals to 0.22–0.28). Watersheds 1, 2, 4 and 10 fall in class 3 (R_c equals to 0.29–0.35).

Lower values of R_f (0.12–0.25) for watersheds 6, 7 and 9 (class 1) signify the tectonic activeness. Higher values of R_f (0.40–0.53) for watersheds 1, 2 and 3 (class 3) indicate practically less tectonic control. Watersheds 4, 5, 8 and 10 (class 2) are under moderate tectonic influence with R_f ranging from 0.26 to 0.39.

Watershed 2 has the lowest value of B_s (1.1–1.5), indicating minimum tectonic influence (class 3). Watersheds 4, 6, 7 and 9 are clubbed into class 1 ($B_s \geq 2.1$), followed by watersheds 1, 3, 5, 8 and 10 (class 2, B_s equals to 1.6–2.0). This indicates relatively moderate tectonic effects in those watersheds. Higher B_s values (> 2.1) in watersheds 4, 6, 7 and 9 indicate active tectonics (class 1). Watersheds 1, 3, 5, 8 and 10 are under the intermediate range (class 2, B_s equals to 1.6–2.0). Only watershed 2 belongs to class 3 with B_s ranging from 1.1 to 1.5, indicating its tectonic activity is minimum.

Master streams of watersheds 3, 4, 7, 8, 9 and 10 show higher values of T. This suggests a higher deflection of the master stream from the theoretical watershed mid-line. It indicates a higher possibility of tectonic effect on these watersheds (class 1, T equals to 0.39–0.52). On the other hand, watersheds 1, 2 and 6 belonging to class 2 indicate lesser possible tectonic influence (T equals to 0.27–0.3), followed by watershed 5 (class 3, T equals to 0.15–0.26).

As per the analysis, watersheds 7, 8 and 9 are tectonically highly active. Watersheds 1, 4–6 and 10 are moderately active. Watersheds 2 and 3 are located in the western part of the study area, where tectonic activity is less intense. The northern portion of the study area in watersheds 6–10 experiences abundant earthquakes indicating active tectonics (Fig. 6). There are several structural lineaments in this northern zone, which includes watersheds 6–10.

IAT map with compiled tectonic information from previous authors clearly shows that (i) tectonically active regions (watersheds 7–9) are characterized by the presence of faults, which could be related to the NKFS. These three watersheds are beside the NKFS, and major structural elements parallel the NKFS. Regional NKFS can influence the surroundings. (ii) Tectonically low active regions are distinguished by fewer structural lineaments/faults. For example, the central part of Saurashtra is less active as watershed 3 shows high R_e (0.72), low R_f (0.004), moderate H_d (0.21) and low HI (0.48). It suggests that the area achieved enough time to expand the watershed laterally, acquiring its circular shape without any tectonic disturbances. Secondly, several localized lineaments do not control the drainage lines. This is evident from the rose diagram for watershed 3 (Fig. 6). Here, the drainage lines are almost equally distributed along several directions. Only shorter NNW-SSE lineaments are found. The entire section of watershed 3 consists of Dwarka Formation and forms a pinnate drainage pattern. This is closely related to a uniform lithology that created an irregular tree branch-shaped drainage pattern.

Table 10
The classification of tectonic activeness among the watersheds.

Class	Range	Tectonic Activity	Watershed
Class 1	1.50–1.80	High	WS 7, 8, and 9
Class 2	1.81–2.11	Moderate	WS 1, 4, 5, 6, and 10
Class 3	2.12–2.42	Low	WS 2 and 3

5.2. Linear parameters

Longitudinal profiles of the master streams of each watershed are prepared from elevation and distance data for a better understanding of the variation in SL index and SI values (Figs. 7 and 8). Evaluated values of these parameters strongly correlate with the tectonic sensitivity of the area. Within the overall sinuous channels with SI (1.0–1.5), the straight channel segments with SI (1.0–1.1) possibly indicate vertical incision due to increased tectonic activity. Knickpoints of each master stream (Fig. 1) are obtained from the longitudinal profile of the corresponding master stream. Master stream 1 has two identifiable knickpoints (Fig. 7). The second knickpoint from the source of this master stream is tectonically significant. This is because the river straightens after crossing this point. The SL index of master stream 1 shows very low values after crossing a structural lineament.

The master stream 2 is dominantly sinuous, but its SI decreases near the knickpoints indicatinga straighter (SI equals to1.00–1.08) flow path. A higher SL index in those regions also indicates vertical incision rather than lateral erosion. The second knickpoint from the upstream side of the master stream 3 is tectonically highly influenced as the stream straightens (SI = 1.09), and higher SL values (65.43) represent more vertical incision. Master stream 4 is completely sinuous, but knickpoint locations indicate the zones of possible active area. Master stream 5 is sinuous but structurally controlled as it parallels the local structural lineaments. Its higher SL indices (85.49, 72.49 and 58.49) characterize three knickpoint locations (Fig. 7). Fault/structural lineament crossing zone in segment 8 of master stream 5 is also supported by the higher SL values (67.09).

SI values display that the master stream 6 is a sinuous channel. However, towards the mouth, it loses power and meanders. The higher SL index values and fault/major lineament crossing this watershed (Fig. 8) developed slope-break and knickpoints due to vertical incision. Master stream 7 shows the alternate straight, sinuous and meandering course. Such alternating channel behavior is the result of episodic uplift/incision. This justifies several tectonic events imprinted on the channel and the incision that occurred due to the presence of faults/lineaments. A lower SI value indicates a straighter channel. It strongly supports the structural control near

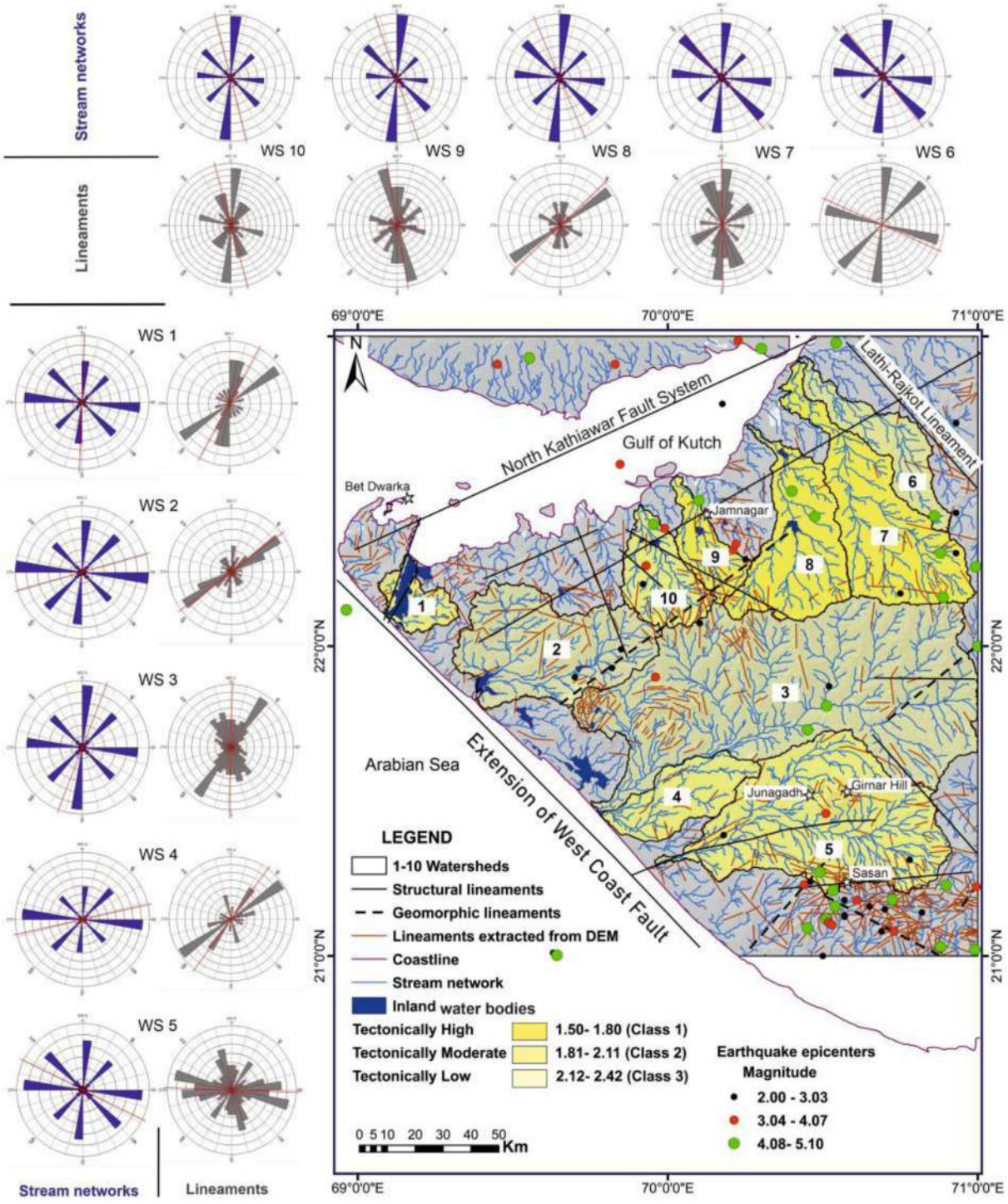

Fig. 6. IAT map where watersheds 7,8 and 9 are tectonically highly active, followed by watersheds 1, 4, 5, 6 and 10. Watersheds 2 and 3 are less active. Major structural lineaments, faults, geomorphic lineaments and lineaments extracted from the DEM and earthquake epicenters are also plotted. Earthquake epicenters [22] are distributed along the structural lineaments and faults. Those regions are tectonically more active as per IAT analysis in this work. Lineament orientations of ten watersheds are represented by grey rose diagrams, prepared using RockWorks 20 software, 2022. The direction of flow path distribution of stream networks of all watersheds represented by blue rose diagrams, prepared using RockWorks 20 software, 2022.

the knickpoints and the structural lineament crossing points. Fieldwork supports that on a uniform basaltic basement, knickpoints developed along the channel due to the presence of faults. Climate acts as a factor of water volume during monsoon. High velocity, discharge stream power and shear stress augment erodibity [60].

Master stream 8 is sinuous towards both source and mouth, but is straight between them. Knickpoints and lineaments are close-spaced. More lineament crossing zones and knickpoints display the higher tectonic activity in watershed 9. Higher SL value (57.9) in fault crossing zones and knickpoint zones in master stream 9 possibly indicates a more tectonic control on the channel flow path

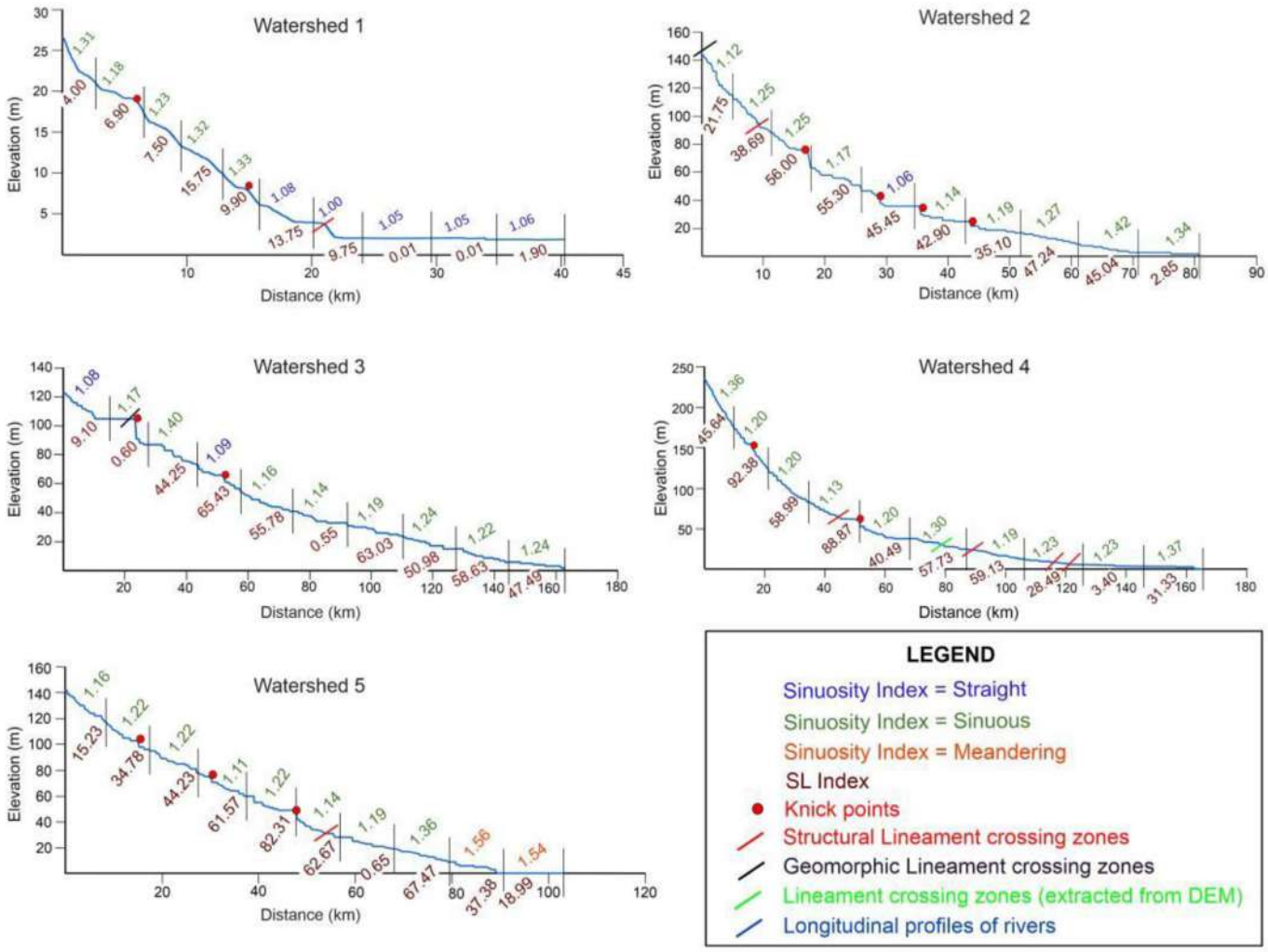

Fig. 7. Source-to-mouth length profiles of the master streams (watersheds 1–5) with the displayed segment-wise SI and SL index values. Sinuosity variation is shown by different colors. Lineaments (extracted from DEM) and knickpoints are plotted. A strong correlation exists among the SI and SL index, lineaments and knickpoint positions.

(Fig. 8). All the knickpoint positions in master stream 10 are supported by the straight nature of the channel (SI < 1.1), indicating higher vertical incision than the lateral (Fig. 8). Lineaments crossing points and knickpoints signify slope-break where rapids, plunge pools and pot-holes developed recently.

Lower values of the Concavity Index (Θ) of the master streams 5–10 indicate that they are tectonically influenced. Therefore, they show the trend of convexity, i.e., vertical erodibility. Vertical incision helps to make the drainage line straighter (less SI value). As per higher values of Θ (0.0119–0.0275), master streams 1–3 have minimum possible influence, indicating higher lateral expansion than vertical incision towards the river mouth. Master streams 4 and 7 show an intermediate range of Θ (0.0056–0.0063), which indicates that the master streams are moderately active. Basin-scale IAT analyses compared to linear-scale Θ values show higher tectonic activity in the northern part and lower tectonic activity in the western to southwestern areas (Fig. 6).

5.3. Analysis of best-fit curve of longitudinal profiles of master streams

The difference between the highest and the linear values of R^2 indicates different degrees of tectonic activity for different watersheds (Table 8). Each master stream is ranked as per the evaluated difference between the highest R^2 and linear R^2 value. The lower the difference, the higher the tectonic influence. For the highest influence, i.e., for the lowest difference, the watershed is ranked as 1. The highest difference of magnitude 0.9967 represents the channel of watershed 5 to be least active, which is ranked as 9. As per the analysis, watersheds 6 and 7 are highly active when the highest R^2 and the linear R^2 are equal (rank 1). This is followed by watersheds 3, 10, 8, 9, 2, 4 and 1 (Table 8). IAT analysis indicates that watersheds 7, 8 and 9 are highly active, whereas watersheds 2 and 3 are characterized by relatively lesser tectonic activity.

Therefore, the results from the analyses of IAT and R^2 curve fitting do not vary much and show a convincing trend of the relative influence of active tectonics except the watershed 3 and the master stream 3. Watershed 3 is tectonically inactive (Table 9), whereas master stream 3 indicates higher tectonic control as per the rank of R^2 curve fitting value analysis (Table 8). Hence, watershed 3 is subcircular, but the master stream is tectonically influenced. This indicates that the zone got enough time to erode the topography to make the watershed circular, but several lineaments and recent tectonic activities affected the master stream to be more active. The overall trend of relative tectonic activity from the R^2 curve fitting is satisfied by the concavity index (Θ) analysis. Comparison of normalized steepness index (K_{sn}) values of ten watersheds with SL, SI and Θ discloses that watersheds 6, 7 and 9 have the highest K_{sn} of

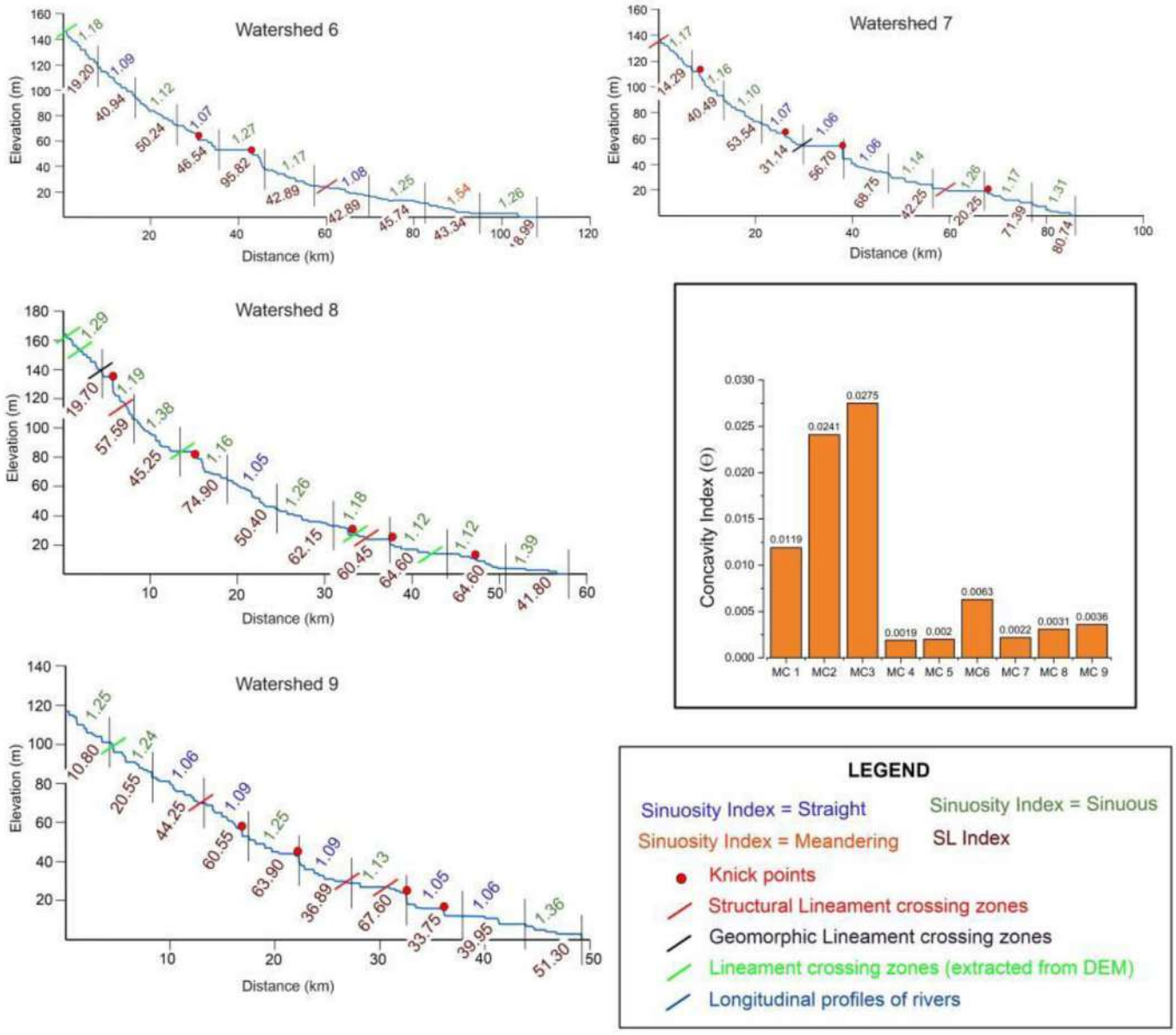

Fig. 8. Source-to-mouth length profiles of master streams in watersheds 6–10 with segment-wise SI and SL. Structural lineaments, geomorphic lineaments and lineaments extracted from DEM and knickpoints are shown. The bar diagram represents Θ of the master streams.

13.20, 0.74 and 1.16, respectively. These watersheds are under active tectonic classes 1 and 2, and the master streams are mostly under sinuous to straight pattern. It is followed by watersheds 5, 8 and 10. Low k_{sn} values indicate a relatively low uplift rate over the watersheds 1 (k_{sn} = 0.11), 2 (k_{sn} = 0.29), 3 (k_{sn} = 0.13) and 4 (k_{sn} = 0.23).

5.4. Seismicity & paleoseismic evidence

IAT analysis, linear parameter study and R^2 curve fitting values indicate an overall higher tectonic activity towards the northern side around Jamnagar (Fig. 9). Numerous earthquakes in the recent past in north Saurashtra corroborate this. The frequency–magnitude relation (b-value) and fractal correlation dimensions (D_c) from 2006 to 2011 [61] disclose that the Kutch rift near the Saurashtra horst zone is active with the average b-value (0.7 ± 0.04) and D_c (2.46 ± 0.01). The hypocenters of the Saurashtra seismic cluster at 5–10 km depth and justify the active tectonics [62].

Watersheds 2 and 3 are tectonically less active, located between the two tectonically highly active regions, i.e., northern- and south-eastern parts of the study area. This detached the Bet Dwarka region from the mainland about 1000 years ago [7]. However, no seismicity has been reported from the Bet Dwarka area in the last few hundred years. The May 2020 earthquake, occurred approximately 13 km south of Dwarka, was about 4.1 magnitudes with approximately 10 km deep focus (Fig. 9). Mandal et al. also suggested the occurrence of a paleo-earthquake presumably 2000 years back around Bet Dwarka [63,64]. This is evidenced by

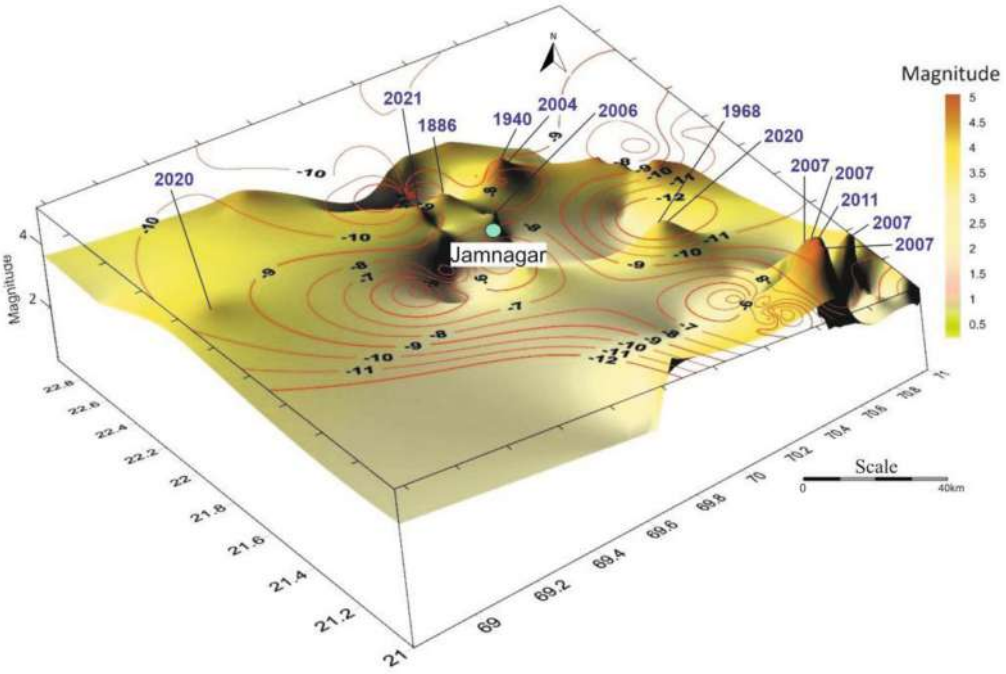

Fig. 9. Spatial variation of earthquake magnitude from 1872 to 2021 [21]. Contours represent depth in km.

seismicity-induced sand blow structures [65]. Additionally, Merh et al. referred to liquefied material in Bet Dwarka, indicating tectonics about 1980 ± 40 yrs BP [66–68]. Geodetic analysis of Saurashtra defines a significant deformation with up to 5.0 ± 2.0 mm y^{-1} rate at several places. The Global Navigation Satellite System (GNSS) study constrains the horizontal movements of less than 1.0 ± 0.4 mm y^{-1} and vertical movements up to 2.3 ± 0.5 mm y^{-1} in the study area [69, 70].

The elongated nature of watersheds on the northern side and the circular watersheds on the southern side indicate more tectonic uplift in the northern portion [71–73]. The concentration of earthquake epicenters in the northern part indicates the same. Rose diagrams of lineament and drainage orientation in Fig. 6 show that rivers flowing to the north follow the same trend as the lineaments. This also indicates tectonically-controlled drainage [71].

5.5. Field verifications

Fieldwork was conducted in watershed 9 (Figs. 10A and 10B). The field locates in the Dhanda village (Fig. 1), about 23 km south of Jamnagar, where the master stream 9 flows. Significant heights of knickpoints and cliff sections indicate tectonic uplift and rejuvenation of the river channel (Figs. 10C, 10D and 10E). Lineaments extracted from DEM are identified at the micro-scale by hill shades [53]. Field verifications also support this: (i) potholes of different sizes (diameter about 0.2–2.5 m, depth about 0.1–1.5 m) (Figs. 10F and 10H); and (ii) the break slope of the cliff section away from the knickpoint locations (Fig. 10G). Potholes can be formed by increased river discharge during heavy precipitation. Potholes can also be caused by an increase in slope induced adjacent to knickpoints, which increases the stream's power and accelerates abrasion/corrosion [73]. Potholes in the study area may indicate recent tectonic activity [74] (Fig. 11A, B, C and D).

Field verification confirms that the northern part of Sautrashtra is tectonically active. The tectonically active zone was possibly responsible for the uplift and inundation of the western tip of the Saurashtra peninsula.

5.6. Other issues

The active faults' uplift rates indicate that Kutch has a complicated geologic history, at least during the Quaternary. The vertical uplift rates, ranging from 0.8 to 2.8 mm y^{-1}, suggest that the KRB has a varied tectonic compressive stress regime [75].

NKFS has an interesting position in the western part of Saurashtra (Fig. 3). Previous researches and the present study prove that the NKFS has been active in the recent past, which is supported by sudden changes in river course in watersheds 6–8 [19]. Hence, NKFS possibly reactivated and submerged/uplifted the western tip of the Saurashtra peninsula. The following evidence supports this.

(1) Coastal cliffs of Dwarka dominated E-W and ENE–WSW (Fig. 2). The region usually consists of vertical joints. There are a few NW-SE trending joints as well. ENE – WSW to E-W and NW- SE joints can be inferred to be related to the NKFS system and the extension of West Coast Fault tectonics, respectively. Towards south from Dwarka along the coastal belt, NW-SE joints are documented dominantly. This indicates the diminished influence of NKFS towards the south. NKFS mainly affected rocks in and around Dwarka.

Fig. 10. (A) Knickpoint locations (white stars) in master stream of watershed 9 and the surrounding regions (Google Earth image acquired on 11-Feb-2022). (B) Zoomed in view around Dhanda village shows two knickpoints. (C) Aerial view of knickpoint 1 (Google Earth image acquired on 11-Feb-2022). (D) Upstream view of master stream of watershed 8 shows knickpoint 1, about 4 m height (Bikramaditya Mondal (BM) marked in a red ellipse, height about 1.65 m). (E) Downstream view of master stream of watershed 8, photo taken from the top of the knickpoint 1 (BM marked in a red ellipse, height about 1.65 m). (F) and (H) Large-scale pothole atop the knickpoint indicating tectonic uplift of the area and rejuvenation of the river channel (notebook marked in a green ellipse, length about 22 cm). (G) Cliff section height decreases gradually from the knickpoint zone (BM marked in a red ellipse, height about 1.65 m).

(2) Focal mechanism of earthquake suggests that the northern part of Saurashtra is dominated by ESE-WNW trending reverse faults and the Saurashtra region is dominated by NE-trending strike-slip faults under transtension [76]. Hence, the stress regime is dissimilar in northern and southern Saurashtra, with vertical movements plausible in the north region. Along the active faults, brittle-ductile transition (BDT) acted as a lubricant for the emergence and triggering of the earthquake. Fluid migration deteriorates the fractured ductile crust by increasing its fluid pressure, which minimizes the confining pressure and endorses velocity weakening in the seismic layer. The resulting shear instability triggered deep crustal earthquakes [77]. This probably contributed to the uplift and inundation of the ancient city Dwarka and the surrounding regions.

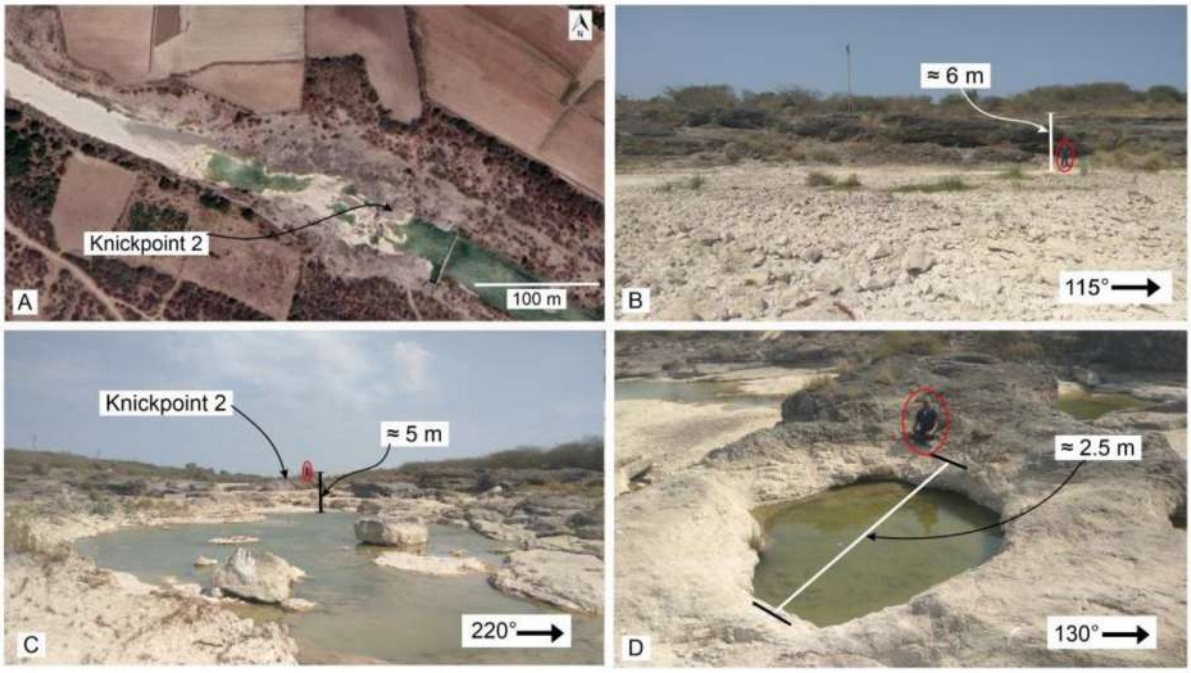

Fig. 11. (A) Aerial view of knickpoint 2 (Google Earth image acquired on 11-Feb-2022). (B) Approximately 6 m high cliff section near the knickpoint 2. (C) Upstream view of the master stream of watershed 8 showing the knickpoint 1 with height about 5 m. (D) A large pothole atop indicating tectonic uplift of the area and rejuvenation of the river channel. (B)–(D): BM marked in a red ellipse, height about 1.65 m.

6. Conclusions

The North Kathiawar Fault System (NKFS) has been tectonically impacting the northern part of Saurashtra, including Jamnagar and the surrounding regions. Watersheds 2, 3 and 5 with westward flowing streams are circular, revealing lateral erosion stronger than the vertical one. The majority of the northward flowing streams in these watersheds are elongated and tectonically active (class 1). Straight channels imply significant vertical incision in watersheds 6–9. The active tectonics can be indicated by potholes recorded in these watersheds, the break of slope points and knickpoints. Saurashtra's northern region is more tectonically active than the southwest portion. The western flank of the Saurashtra may be submerged during NKFS activation.

Conflicts of interest

The authors declare that there is no conflicts of interest.

Acknowledgements

This work was the M.Tech. dissertation of BM under SM in 2022. Internal evaluators Profs. M Mukul and M Radhakrishna (IIT Bombay) commented. The Chief Editor Yiyan Zhou and three anonymous reviewers are thanked for providing review comments in two rounds. This article is dedicated to Prof. L.S. Chamiyal and D.M. Maurya (MS University Baroda), who have contributed significantly to western India's geomorphology. Research Development Fund (IIT Bombay) supported SM.

Appendix-1(Sea-level changes)

The Kutch-Saurashtra region underwent a possible regression in Pliocene to Early Pleistocene and two transgressions in the mid Pleistocene and early Holocene [66,67]. Evidence also shows that the sea level was about 40 m deep relative to the present-day level [14]. As per the sea-level change curve of the India's western continental margin [18], the sea was 100 m deeper than the present-day level (about 14,500 BP), and it rose to approximately 80 m depth (about 12,000 BP). The rate of sea-level rise was about 10 m per 1000 yrs at the mentioned time gap.

The Indian western continental margin has not suffered major sea-level changes in the 2000 years during 12,000–10000 BP, which was followed by a very high rate of rising (about 20 m per 1000 yrs) from 1000 years to 7000 yrs BP [11]. After 7000 years BP, minor fluctuations were documented. The Gulf of Kutch suffered earlier submergence (at least by 15 ka) than the other regions (12–6 ka). After the Last Glacial Maximum (20 ky), the zone further uplifted and subsided during the Holocene [12]. [15] suggested that the southern and the western Saurashtra coasts are stable, at least for the last 4000 years, whereas the shoreline in the Gulf of Khambhat is presently receding. The Great Rann of Kutch was navigable during the Harappan period [16]. Harappan civilization was probably affected by the siltation of the area.

Thermoluminescence (TL) dating of the submerged potsherds in the Bet Dwarka suggests different age ranges: 3870–2220, 3160–830, 1780–960 and 1240-880 years BP, at different locations. Though age ranges varied, when ages are correlated with the locations, they are in conformity with the expected period [13]. [13] considered shoreline change since 2000–3000 years BP in Bet Dwarka. Sea level during mid-Holocene was 2–6 m higher, later, it decreased and about 1000 years BP sea level increased. The later submerged several historic sites [11]. Gaur et al. [16] used archeologic proxies to understand the shoreline changes and concluded that.

i. During Harrapan time:
   a) The shoreline was landward in the Gulf of Khambat.
   b) Possibly Rann of Kutch was navigable.

c) Not much shoreline changes along the southern and western coastline of Saurashtra.

ii. During the early historic period (4th BCE to 4th CE):
   a) The sea level was lower about 2 m in Bet Dwarka and the northern coast of Saurashtra.

iii. During medieval period:
   a) Shoreline advanced and the temple at Pindara submerged.

Appendix-2

Geomorphologically Saurashtra peninsula can be subdivided into five categories of landforms [19] viz., (i) denudational landform/dissected plateau (mainly occupied by Deccan volcanics of 37,462 km^2), (ii) geological features such as dykes, fault scarp, fault line scarp (750 km^2), (iii) Coastal landforms (7100 km^2), (iv) Aeolian landform (2780 km^2) and (v) Fluvial landforms (1505 km^2).

References

[1] S.S. Merh, Geology of Gujarat, Geological Society of India, Bangalore, 1995.
[2] K. Sriram, S.S. Gupte, V. Kothari, M. Bisen, R.S. Waraich, Structure and evolution of Saurashtra arch in Kutch-Saurashtra deepwater area, western India, in: 6th International conference & exposition on petroleum Geophysics, Kolkata, 2006, pp. 21–25.
[3] J.N. Malik, P.S. Sohoni, S.S. Merh, R.V. Karanth, Active tectonic control on alluvial fan architecture along Kachchh mainland Hill Range, Western India, Z. Geomorphol. (2001) 81–100.
[4] S.N. Bhattacharya, R.V. Karanth, R.S. Dattatrayam, P.S. Sohoni, Earthquake sequence in and around Bhavnagar, Saurashtra, western India during August–December 2000 and associated tectonic features, Curr. Sci. 86 (2004) 1165–1170.
[5] B.K. Rastogi, S. Kumar, S.K. Aggrawal, K. Mohan, N. Rao, N.P. Rao, G.C. Kothyari, The October 20, 2011 Mw 5.1 Talala earthquake in the stable continental region of India, Nat. Hazards 65 (2013) 1197–1216.
[6] N. Vanik, M.A. Shaikh, S. Mukherjee, D.M. Maurya, L.S. Chamyal, Post-Deccan Trap stress reorientation under transpression: evidence from fault slip analyses from SW Saurashtra, Western India, J. Geodyn. 121 (2018) 9–19.
[7] U. Bhonde, N. Bhatt, Joints as fingerprints of stress in the quaternary carbonate deposits along coastal Saurashtra, Western India, J. Geol. Soc. India 74 (2009) 703–710.
[8] A.S. Gaur, K.H. Vora, Shoreline changes during the last 2000 years on the Saurashtra coast of India: study based on archaeological evidences, Curr. Sci. 92 (2007) 103–110.
[9] N. Bhatt, Lithostratigraphy of the neogene-quaternary deposits of Dwarka-Okha area, Gujarat, J. Geol. Soc. India 55 (2000) 139–148.
[10] A.S. Gaur, S. Tripati, S. Tripati, An ancient harbour at Dwarka: study based on the recent underwater explorations, Curr. Sci. 86 (2004) 1256–1260.
[11] N.H. Hashimi, R. Nigam, R.R. Nair, G. Rajagopalan, Holocene sea level fluctuations on western Indian continental margin: an update, J. Geol. Soc. India 46 (1995) 157–162.
[12] V.P. Rao, M. Veerayya, M. Thamban, B.G. Wagle, Evidences of late Quaternary neotectonic activity and sea-level changes along the Western Continental margin of India, Curr. Sci. (1996) 213–219.
[13] K.H. Vora, A.S. Gaur, D. Price, Sundaresh, Cultural sequence of Bet Dwarka island based on thermoluminescence dating, Curr. Sci. 82 (2002) 1351–1356.
[14] V.P. Rao, G. Rajagopalan, K.H. Vora, F. Almeida, Late Quaternary sea level and environmental changes from relic carbonate deposits of the western margin of India, J. Earth Syst. Sci. 112 (2003) 1–25.
[15] K.H. Vora, A.S. Gaur, S. Tripati, Archaeological sites as indicators of ancient shorelines, in: A.S. Gaur, K.S. Vora (Eds.), Glimpses of marine archaeology in India, National Institute of Oceanography, 2006, pp. 82–86, 9788190007429.
[16] A.S. Gaur, Sundaresh, Palaeo-coastline of Saurashtra, Gujarat: a study based on archaeological proxies, Indian J. Geo Marine Sci. 43 (2014) 1224–1229.
[17] L. Michael, D.G. Rao, K.S. Krishna, K.H. Vora, Late Quaternary seismic sequence stratigraphy of the Gulf of Kachchh, northwest of India, J. Coast Res. 25 (2009) 459–468.
[18] K. Lambeck, H. Rouby, A. Purcell, Y. Sun, M. Sambridge, Sea level and global ice volumes from the last glacial maximum to the Holocene, Proc. Natl. Acad. Sci. USA 111 (2014) 15296–15303.
[19] S. Das, P.K. Singh, S. Chaudhari, Neotectonic activities in northern Saurashtra peninsula bordering Gulf of kachchh, J. Indian Soc. Remote Sens. 44 (2016) 553–562.
[20] B.G. Desai, Ichnological analysis of the Pleistocene Dwarka Formation, Gulf of kachchh: tracemaker behaviors and reworked traces, Geodin. Acta 28 (2016) 18–33.
[21] N. Vanik, D.M. Maurya, M. Shaikh, A. Padmalal, P. Tiwari, L.S. Chamyal, A tectono-geomorphological perspective of micro-earthquake swarm activity prone areas around Bhavnagar and Jamnagar in Saurashtra, western India, Quat. Int. 585 (2021) 111–133.
[22] https://earthquake.usgs.gov/earthquakes.
[23] https://isr.gujarat.gov.in/sites/default/files/eq_catalogue_gujarat.pdf.
[24] https://isr.gujarat.gov.in/latest-earthquakes-reports.
[25] C. Kamra, S. Chopra, R.B.S. Yadav, Joint inversion for stress and fault orientations using focal mechanisms of earthquakes in the Saurashtra horst, a part of stable continental region of India, and source parameter estimation, J. Seismol. 25 (2021) 1141–1159.
[26] R.S. Kandregula, G.C. Kothyari, K.V. Swamy, S. Rawat, Quantitative assessment of tectonic activity in Northern Saurashtra, Western India, J. Indian Geophys. Union 23 (2019) 542–558.
[27] D. Gandhi, P. Prajapati, S.P. Prizomwala, N. Bhatt, B.K. Rastogi, Delineating the spatial variability in neotectonic activity along southwestern Saurashtra, Western India, Z. Geomorphologie 59 (2015) 21–36.
[28] S.A. Mahmood, R. Gloaguen, Appraisal of active tectonics in hindu Kush: insights from DEM derived geomorphic indices and drainage analysis, Geosci. Front. 3 (2012) 407–428.
[29] H.B. Soni, K. Thakur, Preliminary checklist of marine mollusks from Beyt Dwarka, Gulf of Kutch (eco-sensitive zone), Gujarat, India, Int. J. Environ. 4 (2015) 243–255.
[30] J.P. Narayan, M.L. Sharma, Effects of local geology on damage severity during Bhuj India earthquake, in: 13th World conference on earthquake engineering, 2004.
[31] Sundaresh, A.S. Gaur, Archaeology of Bet Dwarka, Man Environ. 23.2 (1998) 77–86.
[32] K.G. Kulkarni, V.D. Borkar, T. Petare, Gastrochaenolites bioerosion in the Kalyanpur limestone (Pliocene) of Dwarka area, kathiawar, Gujarat, Geol. Soc. India 72 (6) (2008) 774–780.
[33] S.K. Biswas, Regional tectonic framework, structure and evolution of the western marginal basins of India, Tectonophysics 135 (1987) 307–327.
[34] S. Dasgupta, P.L. Narula, S.K. Acharyya, J. Banerjee, Seismotectonic atlas of India and its environs, Geological Survey of India, Kolkata, 2000.
[35] M.V. Sakhawala, D.M. Shringarpure, Age of the Dwarka beds and the subsequent strata at Bet shankhodhar, Gulf of Kutch, Gujarat state, in: Stratigraphic boundary problems in India, Geological Society of India, 1990, pp. 111–116.
[36] O. Heidbach, M. Rajabi, K. Reiter, M. Ziegler, Wsm Team, World stress map database release 2016, 10, GFZ Data Services, 2016.
[37] S.A. Schumm, Evolution of drainage systems and slopes in badlands at Perth Amboy, New Jersey, Geol. Soc. Am. Bull. 67 (1956) 597–646.
[38] A.N. Strahler, Hypsometric (area-altitude) analysis of erosional topography, Geol. Soc. Am. Bull. 63 (1952) 1117–1142.
[39] P.W. Hare, T.W. Gardner, Geomorphic indicators of vertical neotectonism along converging plate margins, Nicoya Peninsula, Costa Rica, Tectonic Geomorphol. 4 (1985) 75–104.
[40] R.E. Horton, Erosional development of streams and their drainage basins; hydrophysical approach to quantitative morphology, Geol. Soc. Am. Bull. 56 (1945) 275–370.
[41] M.T. Ramírez-Herrera, Geomorphic assessment of active tectonics in the Acambay Graben, Mexican volcanic belt, Earth Surf. Process. Landforms: J. Br. Geomorphol. Group 23 (1998) 317–332.
[42] R.T. Cox, Analysis of drainage-basin symmetry as a rapid technique to identify areas of possible Quaternary tilt-block tectonics: an example from the Mississippi Embayment, Geol. Soc. Am. Bull. 106 (1994) 571–581.
[43] V.S. Kale, S. Sengupta, H. Achyuthan, M.K. Jaiswal, Tectonic controls upon Kaveri River drainage, cratonic Peninsular India: inferences from longitudinal profiles, morphotectonic indices, hanging valleys and fluvial records, Geomorphology 227 (2014) 153–165.
[44] M. Biswas, M.P. Gogoi, B. Mondal, T. Sivasankar, S. Mukherjee, S. Dasgupta, Geomorphic assessment of active tectonics in Jaisalmer basin (western Rajasthan, India), Geocarto Int. (2022), https://doi.org/10.1080/10106049.2022.2066726.
[45] M. Biswas, M.K. Puniya, M.P. Gogoi, S. Dasgupta, S. Mukherjee, N.R. Kar, Morphotectonic analysis of petroliferous Barmer rift basin (Rajasthan, India), J. Earth Syst. Sci. 131 (3) (2022) 140.
[46] S. Dasgupta, M. Biswas, S. Mukherjee, R. Chatterjee, Structural evolution and sediment depositional system along the transform margin-Palar–Pennar basin, Indian east coast, J. Petrol. Sci. Eng. 211 (2022) 110–155.
[47] N. Kumar, R.K. Dumka, K. Mohan, S. Chopra, Relative active tectonics evaluation using geomorphic and drainage indices, Dadra Nagar Haveli, western India. Geodesy Geodynamics 13 (3) (2022) 219–229, https://doi.org/10.1016/j.geog.2022.01.001.
[48] T. Solanki, P.M. Solanki, N. Makwana, S. Prizomwala, G.C. Kothyari, Geomorphic response to neotectonic instability in the Deccan volcanic province, Shetrunji River, western India: insights from quantitative geomorphology, Quat. Int. 575 (2021) 96–110, https://doi.org/10.1016/j.quaint.2020.06.015.
[49] J.T. Hack, Stream-profile analysis and stream-gradient index, J. Res. U. S. Geol. Surv. 1 (1973) 421–429.
[50] J.C. Brice, Channel patterns and terraces of the loup rivers in Nebraska, US Government Printing Office, 1964.
[51] K.X. Whipple, C. Wobus, B. Crosby, E. Kirby, D. Sheehan, New tools for quantitative geomorphology: extraction and interpretation of stream profiles from digital topographic data, GSA short course 506 (2007) 1–26.

[52] N.P. Snyder, K.X. Whipple, G.E. Tucker, D.J. Merritts, Landscape response to tectonic forcing: digital elevation modelanalysis of stream profiles in the Mendocino triple junction re-gion, northern California, Geol. Soc. Am. Bull. 112 (2000) 1250–1263, https://doi.org/10.1130/0016-7606(2000)112<1250:lrttfd>2.0.co;2.
[53] C.S. Lee, L.L. Tsai, A quantitative analysis for geomorphic indices of longitudinal river profile: a case study of the Choushui River, Central Taiwan, Environ. Earth Sci. 59 (2010) 1549–1558.
[54] M.D.P. Villalta Echeverria, A.G. Viña Ortega, E. Larreta, P. Romero Crespo, M. Mulas, Lineament extraction from digital terrain derivate model: a case study in the girón–santa isabel basin, south Ecuador, Rem. Sens. 14 (21) (2022) 5400.
[55] E.A. Keller, T.K. Rockwell, Tectonic geomorphology, Quaternary chronology, and paleoseismicity, Dev. Appl.Geomorphol. (1984) 203–239.
[56] S.G. Wells, T.F. Bullard, C.M. Menges, P.G. Drake, P.A. Karas, K.I. Kelson, J.R. Wesling, Regional variations in tectonic geomorphology along a segmented convergent plate boundary pacific coast of Costa Rica, Geomorphology 1 (3) (1988) 239–265.
[57] S. Rhea, Geomorphic observations of rivers in the Oregon Coast Range from a regional reconnaissance perspective, Geomorphology 6 (2) (1993) 135–150.
[58] P.S. Sohoni, J.N. Malik, S.S. Merh, R.V. Karanth, Active tectonics astride katrol hill zone, kachchh, western India, Geol. Soc. India 53 (5) (1999) 579–586.
[59] P.G. Silva, J.L. Goy, C. Zazo, T. Bardajı, Fault-generated mountain fronts in southeast Spain: geomorphologic assessment of tectonic and seismic activity, Geomorphology 50 (1–3) (2003) 203–225.
[60] S. Soni, Assessment of morphometric characteristics of Chakrar watershed in Madhya Pradesh India using geospatial technique, Appl. Water Sci. 7 (2017) 2089–2102, https://doi.org/10.1007/s13201-016-0395-2.
[61] A.P. Singh, I.G. Roy, S. Kumar, et al., Seismic source characteristics in Kachchh and Saurashtra regions of Western India: b-value and fractal dimension mapping of aftershock sequences, Nat. Hazards 77 (Suppl 1) (2015) 33–49, https://doi.org/10.1007/s11069-013-1005-3.
[62] B.K. Rastogi, S. Kumar, S.K. Aggrawal, K. Mohan, N. Rao, N.P. Rao, G.C. Kothyari, The October 20, 2011 Mw 5.1 Talala earthquake in the stable continental region of India, Nat. Hazards 65 (2) (2012) 1197–1216, https://doi.org/10.1007/s11069-012-0226-1.
[63] P. Mandal, R. Narsaiah, B. Sairam, C. Satyamurty, I.P. Raju, Relocation of early and late aftershocks of the 2001 Bhuj earthquake using joint hypocentral determination (JHD) technique: implication toward the continued aftershock activity for more than four years, Pure Appl. Geophys. 163 (2006) 1561–1581.
[64] C.P. Rajendran, K. Rajendran, K.H. Vora, A.S. Gaur, The odds of a seismic source near Dwarka, NW Gujarat: an evaluation based on proxies, Curr. Sci. 84 (2003) 695–701.
[65] K.H. Vora, Marine archaeological investigations in inferring shoreline/sea level changes along the Indian coast, URL, https://drs.nio.org/drs/bitstream/handle/2264/661/Refresher_Course_Mar_Geol_Geophys_2007_Lecture_Notes_177.pdf?sequence=2, 2007. (Accessed 12 May 2022).
[66] S.S. Merh, Neogene-Quaternary sequence in Gujarat: a review, J. Geol. Soc. India 41 (1993) 259–276.
[67] V.S. Krishnaswamy, R.N. Iyengar, B.P. Radhakrishna, Evolution of the western coastline of India and the probable location of dwaraka of krishna: geological perspectives, J.Geol. Soc. India (Online archive from 1 (78) (2005) 778–782, 66.
[68] S.K. Biswas, Rift basins in western margin of India and their hydrocarbon prospects with special reference to Kutch basin, AAPG Bull. 66 (1982) 1497–1513.
[69] G.S.P. Rao, H.C. Tewari, The seismic structure of Saurashtra crust in northwest India and its relationship with the Reunion Plume, Int. J. Geophys. 160 (2005) 318–330.
[70] D. Suribabu, R.K. Dumka, G.C. Kothyari, et al., Identification of crustal deformation in the Saurashtra region, western India: insights from PSI and GNSS derived investigation, Acta Geod Geophys 57 (2022) 639–659, https://doi.org/10.1007/s40328-022-00399-z.
[71] W.B. Bull, L.D. McFadden, Tectonic geomorphology north and south of the Garlock Fault, California, in: D.O. Doehring (Ed.), Geomorphology in arid regions, Publications in Geomorphology, State University of New York at Binghampton, 1977, https://doi.org/10.1007/s13201-016-0524-y.
[72] K. Prakash, T. Mohanty, J.K. Pati, et al., Morphotectonics of the Jamini River basin, Bundelkhand Craton, Central India; using remote sensing and GIS technique, Appl. Water Sci. 7 (7) (2017) 3767–3782, https://doi.org/10.1007/s13201-016-0524-y.
[73] N.S. Withanage, N.D.K. Dayawansa, R.P. De Silva, Morphometric analysis of the Gal Oya River Basin using spatial data derived from GIS, Trop. Agric. Res. 26 (1) (2014) 175–188.
[74] M.K. Dhali, M. Biswas, MCA on mechanism of river bed potholes growth: a study of middle Subarnarekha River basin, South East Asia, Environ. Dev. Sustain. 21 (2019) 935–959.
[75] G.C. Kothyari, R.S. Kandregula, R. Dumka, G. Chauhan, A.K. Taloor, Quaternary tectonic history of seismically active intraplate Kachchh Rift Basin, western India: a review, Geodesy Geodynamics 13 (3) (2022) 192–204, https://doi.org/10.1016/j.geog.2021.09.011.
[76] S. Dasgupta, S. Mukherjee, Brittle shear tectonics in a narrow continental rift: asymmetric nonvolcanic Barmer Basin (Rajasthan, India), J. Geol. 125 (5) (2017) 561–591.
[77] G.C. Kothyari, R.K. Dumka, S. Chopra, K.D. Singh, B.K. Tamta, C. Kamra, Triggering mechanism and brittle-ductile dynamics of active faults in the south-central Saurashtra horst, Gujarat, western India: a geospatial, geological, and geophysical approach, J. Asian Earth Sci. X 9 (2023) 100155, https://doi.org/10.1016/j.jaesx.2023.100155.

Bikramaditya Mondal did Geology Hons. course from Hooghly Mohsin College in 2018. He qualified M.Sc. in Applied Geology from the National Institute of Technology, Rourkela in 2020, and M. Tech. in Petroleum Geoscience from the Indian Institute of Technology Bombay in 2022.

Mery Biswas is an assistant professor in Presidency University, Kolkata. She worked on several aspects/methods of morphotectonics and fluvial geomorphology (field-based, instrumental survey techniques analytical models, micro landforms etc.). She published articles in several international journals.

Soumyajit Mukherjee is a professor in IIT Bombay. Specialization: Structural Geology and tectonics. He is an associate editor in Marine and Petroleum Geology (Elsevier). He teaches structural geology and elementary stratigraphy to students at different levels in IIT Bombay in theory and practical classes and in field. He has published 20 special volumes and books with leading international publishers, as well as over 100 research papers.

Mohamedharoon A. Shaikh did B.Sc. M.Sc. and Ph.D. in Geology from The Maharaja Sayajirao University of Baroda. Presently working as a postdoctoral researcher in IIT Bombay.